^{1}H and ^{7}Li NMR in $Li_{2-x}H_xMO_3$ (M = Ti, Zr)

Ya.V. Baklanova

Institute of Solid State Chemistry, Yekaterinburg 620219, Russia
E-mail: BaklanovaY@ihim.uran.ru

Received April 2, 2008
Revised May 15, 2008
Accepted May 28, 2008

Magnetic Resonance in Solids
Electronic Journal

Volume **10**, *No.* **1**,
pages **39-45**, **2008**

http://mrsej.ksu.ru

^1H and ^7Li NMR in $Li_{2-x}H_xMO_3$ (M = Ti, Zr)

Ya.V. Baklanova
Institute of Solid State Chemistry, UB RAS, Pervomaiskaya, 91, Yekaterinburg 620219, Russian Federation
E-mail: BaklanovaY@ihim.uran.ru

Nuclear magnetic resonance (NMR), Raman spectroscopy and thermogravimetric methods were used to study the peculiarities of lithium ion replacement by protons in lithium metallates Li_2MO_3 (M=Ti, Zr). In this article we show that almost all protons in the final substitution products H_2MO_3 enter into the crystal structure. All protons in zirconium hydroxide belong to hydrogen-bonded OH-groups. Contrary, titanium hydroxide contains both hydrogen-bonded and isolated OH-groups. Protons in H_2ZrO_3 form hydrogen bonds weaker than in H_2TiO_3.

PACS: 61.05.Qr, 82.56.Ub, 82.80.Gk

Keywords: nuclear magnetic resonance, hydroxide compounds, titanium dioxide, zirconium dioxide

1. Introduction

The most extensively studied crystal oxyhydrates of IV-group elements are hydrated titanium and zirconium dioxides $MO_2 \cdot H_2O$ (M=Ti, Zr) used as selective sorbents of rare-earth elements [1]. Recently much interest has stemmed to the so-called titanium acids of the composition $H_2Ti_2O_5$, $H_2Ti_3O_7$, $H_2Ti_4O_9$ since it turned out to be possible to synthesize them in the nanotubular state and use them as precursors for photosynthesis catalysts [2].

The aim of this work was to elucidate the peculiarities of lithium ion replacement by protons in Li_2MO_3 and determine the structure of novel compounds H_2MO_3.

2. Experimental

Sample preparation

Lithium salts Li_2MO_3 (M = Zr, Ti) with disordered crystal structure were synthesized by solid phase reaction between lithium carbonate and metal dioxide MO_2 at final annealing temperatures 870 and 970 K respectively. $Li_{2-x}H_xMO_3$ phases ($0 < x \leq 2$) were prepared from Li_2MO_3 through ion exchange in 0.05 M acetic acid at 330 K. The exchange degree beween Li and H ions was varied by the time of processing with acid solution. The final exchange products were novel compositions H_2MO_3 (or $MO(OH)_2$) with individual crystal structure.

Analyses

The chemical composition of the materials was determined using emission spectral analysis. NMR spectra were recorded using a wide-line NMR spectrometer, allowing to register the first derivative of NMR absorption line of the solid sample in a temperature range from 120 to 300 K. Wide-line ^{7}Li, ^{1}H NMR spectra were recorded with working spectrometer frequencies 34 and 90 MHz accordingly.

In order to assign ^{7}Li NMR signals to certain lithium sites in the crystal lattice we have assumed that the electric field gradient (EFG) on lithium nucleus in the first approximation is determined by symmetry distortion of O^{2-} ions environment of Li nuclei in LiO_6 octahedrons. The formula given in [3] has been used for estimation of LiO_6 octahedrons distortion (Table 1).

$$\alpha = \sqrt{\sum_{i=1}^{N} \left| 1 - \frac{R_i}{\overline{R}} \right|^2}, \quad \overline{R} = \sum_{i=1}^{N} \frac{R_i}{N} \qquad (1)$$

where R_i is a distance Li – O in LiO_6 *i*-octahedron, $N = 6$ is the number of octahedron tops.

Distances between atoms in a crystal lattice were calculated using “Atoms” software package on the basis of a priori structural data.

Solid state magic angle spinning nuclear magnetic resonance (SS-MAS-NMR) ^{1}H was carried out using a Bruker MSL-400 NMR spectrometer, the spinning rates were varied from 2 to 15 kHz.

Raman spectra were recorded on a Renishaw-1000 spectrometer (Ar^+-laser, $\lambda = 514.5$ nm) in the region (50 - 4000) cm^{-1}. Thermogravimetric analysis was carried out on a Setaram TG/DTA 92 thermoanalyzer in the air atmosphere; the balance sensitivity was $10^{-6}\,g$.

Table 1. *Values of quadrupole frequency (ν_Q) and integral intensity (S) of different NMR spectra components of Li_2MO_3 compounds (M=Ti, Zr)*

Compound	Li fraction in the *i*-th site	LiO_6 octahedra distortions α, arb. units	ν_Q, kHz	S, % (± 5)
Li_2TiO_3	Li1 - 50%	0.069	21.0	74.3
	Li2 - 25%	0.076		
	Li3 - 25%	0.243	44.5	25.7
Li_2ZrO_3	Li1 - 50%	0.166	51.5	51.4
	Li2 - 50%	0.050	28.5	48.6
$Li_{0.3}H_{1.7}ZrO_3$	-	-	49	31,6
	-	-	26	68,4

3. Crystal structures of Li_2MO_3

The ordered crystal lattices of lithium metallates Li_2MO_3 (M = Ti, Zr) are derivatives from the rock salt lattice (space group C2/c) with monoclinic distortion. In the crystal lattice of lithium titanate Li_2TiO_3, Li^+ ions occupy octahedral sites Li(1), Li(2) between layers of TiO_6 octahedra and Li(3) sites located in these layers (Fig.1a) [4]. In the monoclinic lithium zirconate Li_2ZrO_3, octahedral sites in the cubic close packing of oxygen ions are occupied by lithium Li(1), Li(2) and zirconium ions, i.e. layers perpendicular to the *c* axis have the same ratio of Li^+ and Zr^{4+} ions equal to 2:1 [5]. (Fig. 1b.).

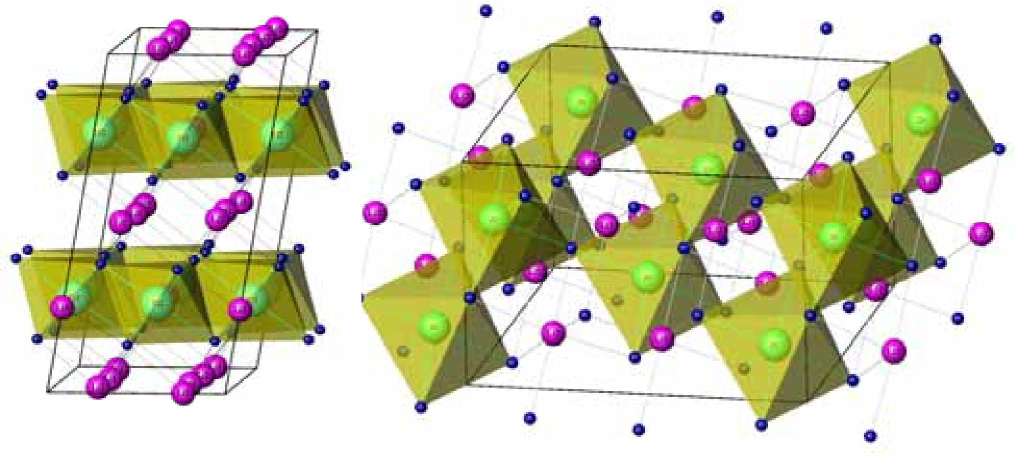

(*a*) (*b*)

Fig. 1. Crystal lattices structure of Li_2MO_3, M = Ti (*a*), Zr (*b*).

4. Results

^{7}Li NMR spectra of $Li_{2-x}H_xMO_3$

As nuclear spin of ^{7}Li is 3/2, i.e. the lithium nucleus has quadrupole moment, therefore central lines and two satellite lines are observed on NMR ^{7}Li spectra. Quadrupole frequency is defined as the distance between satellites and depends on EGF value [6].

NMR spectra of $Li_{2-x}H_xZrO_3$ compounds were decomposed in the "Simul" software packet into two components having almost the similar values of related intensity and different values of quadrupole frequency, in accordance with two lithium sites Li(1) and Li(2). The NMR spectrum of Li_2TiO_3 samples was decomposed into two components: the first line can be attributed to Li(1) and Li(2) sites and the second one can be linked to Li(3) sites (Fig. 2.). Values of quadrupole frequency and integral intensity of contributions from different lithium sites are listed in Table 1.

^{1}H NMR spectra of H_2MO_3

Wide-line ^{1}H NMR spectra recorded as first derivatives of an absorption lines have symmetric forms relative of signal centers. So in Fig. 3 only one halfs of spectra are shown. At 130 K spectra have a form of a wide single line from protons of structural OH-group. Parameters of half-width lines (Δh) are equal $(3.0 - 4.5)\cdot 10^{-4}$ T. At temperature 300 K the narrow lines ($\Delta h = 0.5\cdot 10^{-4}$ T) from absorbed water molecules are observed whereas the spectra from protons of OH-groups remains constant.

^{1}H-MAS-NMR spectra of $Li_{2-x}H_xMO_3$

The ^{1}H NMR spectra of $Li_1H_1TiO_3$ and H_2TiO_3 samples may be represented as a supersposition of two lines with different values of signal chemical shift relative to TMS (tetramethilsilan) [7]: $\delta_1 = 5.7$ ppm, $\delta_2 = 9.7$ ppm for the intermediate composition $Li_1H_1TiO_3$, and $\delta_1 = 5.8$ ppm, $\delta_2 = 11.4$ ppm for H_2TiO_3 (Fig. 4). The chemical shift value for ^{1}H NMR spectra of H_2ZrO_3 samples is 7.5 ppm (Fig. 5).

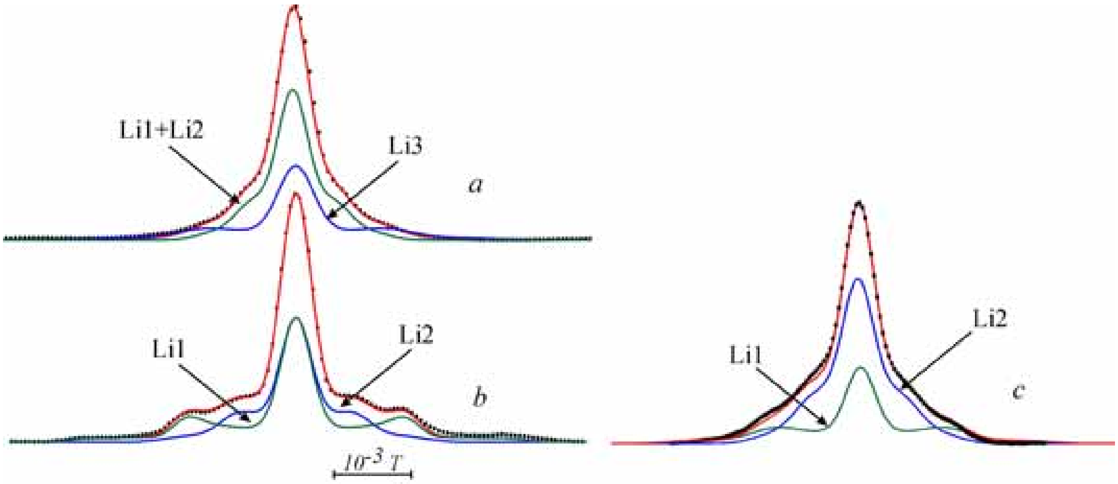

Fig. 2. Experimental (dots) and calculated (red line) ^{7}Li NMR spectra of Li_2TiO_3 (*a*), Li_2ZrO_3 (*b*), $Li_{0.3}H_{1.7}ZrO_3$ (*c*) compounds; arrows indicate components from different lithium sites.

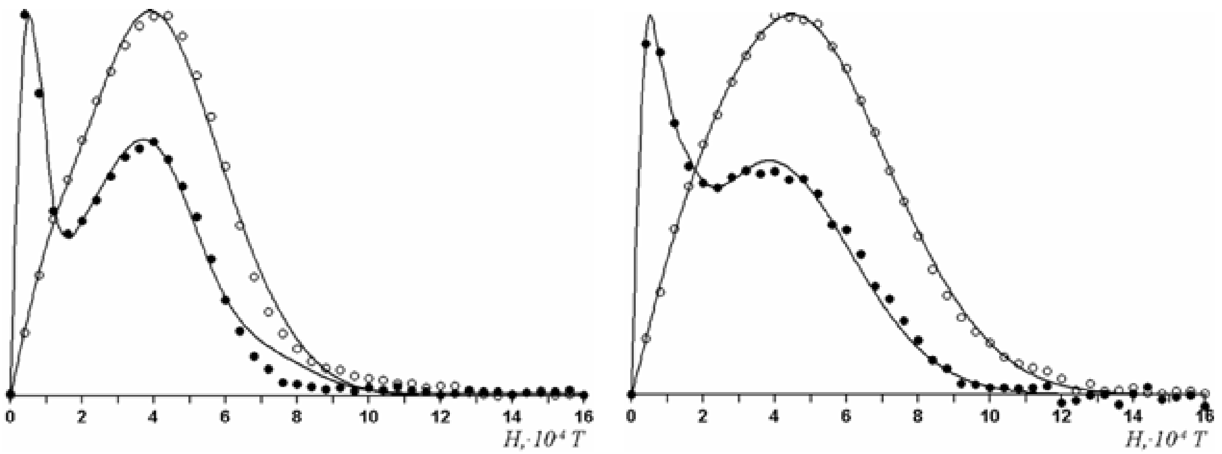

(*a*) (*b*)

Fig. 3. Experimental (dots) and calculated (solid lines) ^{1}H NMR wide-line spectra: H_2TiO_3 (*a*), H_2ZrO_3 (*b*); (○) - 130 K, (●) - 300 K.

Raman spectra of H_2MO_3

Raman scattering lines on the spectra of H_2MO_3 in the interval 130-900 cm^{-1} are assigned to stretching and deformation vibrations of metal-oxygen bonds [8]. In the region of stretching vibrations of O-H bonds (2500 – 4000) cm^{-1}, two lines at 3100 cm^{-1} and 3500 cm^{-1} are observed on the spectrum of H_2TiO_3. On the spectrum of H_2ZrO_3, in the region of stretching vibrations of O-H bonds (3000 – 4000) cm^{-1} a wide asymmetric line is observed at 3400 cm^{-1} (Fig. 6).

TDG curves of H_2MO_3 compounds

Decomposition effect extrema for H_2TiO_3 and H_2ZrO_3 lie in the range (420 – 440) K and (450 – 470) K, respectively, (Fig. 7) depending on the sample's heating rate.

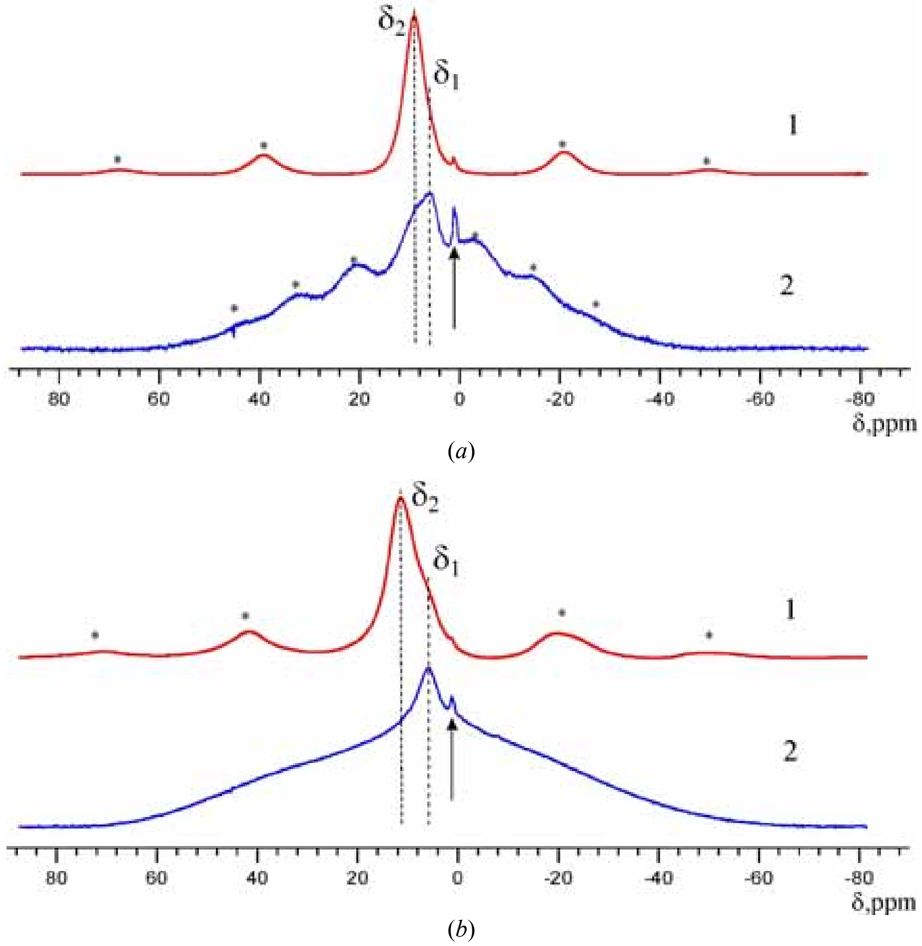

(*a*)

(*b*)

Fig. 4. ^{1}H-MAS-NMR spectra: $Li_1H_1TiO_3$ (*a*) (at spinning rates: 1 – 12 kHz, 2 – 4.5 kHz); H_2TiO_3 (*b*) (at rotation rates: 1 – 12 kHz, 2 – static spectrum). Dashed lines designate isotropic lines, arrows denote PMR detector signals, stars (*) show the side bands arising while the sample is rotating in the magnetic feild.

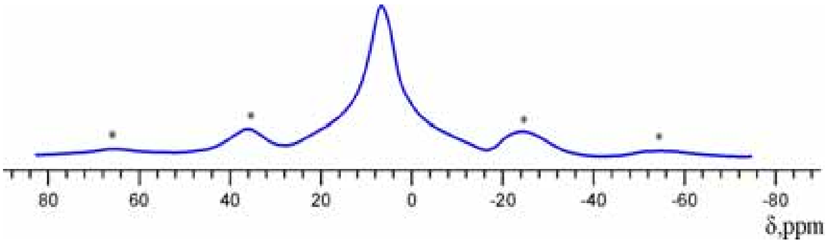

Fig. 5. ^{1}H-MAS-NMR spectra of the H_2ZrO_3 sample at spinning rate 12 kHz, stars (*) show the side bands arising while the sample is rotating in the magnetic feild.

5. Discussion

As follows from the data in Table 1, the areas under the signals from lithium nuclei with different EFG values coincide with the relative population of the corresponding lithium sites in the crystal lattice of the compounds (Table 1). The intensity of the line from the Li(1) site in the spectrum of $Li_{0.3}H_{1.7}ZrO_3$ decreases in comparison with the same of Li_2ZrO_3 (Fig. 2b,c). It can be suggested that the Li(1) site is more preferable for replacement by protons than the Li(2) site, *i.e.* Li^+ for H^+ ion exchange in lithium zirconate begins with Li(1) sites.

H_2MO_3 wide-line ^{1}H NMR spectra differ essentially from resonance signals of hydrated dioxide $MO_2{\cdot}H_2O$ samples [1]. The lines with $\Delta h = (3.0 - 4.5){\cdot}10^{-4}$ T does not depend on temperature, and they may be attributed to protons in the the crystal structure of the compounds. H_2MO_3 wide-line ^{1}H NMR spectra differ essentially from resonance signals of hydrated dioxide $MO_2{\cdot}H_2O$ samples [1]. The lines with $\Delta h = (3.0 - 4.5){\cdot}10^{-4}$ T does not depend on temperature, and they may be attributed to protons in the the crystal structure of the compounds. At temperature 300 K a narrow line from water molecules is observed (Fig. 3). The relative content of protons of adsorbed H_2O is less than 5 %.

High-resolution NMR spectra allow establishing differences in the states of structural protons in titanium hydroxides H_2TiO_3 (Fig. 4). The fact that two lines with different chemical shift values are present in the spectrum indicates non-equivalent sites of protons. When going from $Li_1H_1TiO_3$ to H_2TiO_3, the chemical shift value of the most intense (δ_2) increases. This testifies that the degree of hydrogen nucleus screening decreases as a result of formation of hydrogen bonds. The low-intensity signal has almost the same chemical shift value and is attributed to protons of isolated OH groups having no hydrogen bonds.

Since the value of ∂ in NMR spectra of H_2ZrO_3 is less than the value of δ_2 in H_2TiO_3, it may be concluded that protons in zirconium hydroxide are much stronger bonded and, consequently, hydrogen bonds are weaker than in titanium hydroxide.

Our NMR findings are supplemented by Raman spectroscopy data. Raman scattering lines in the range 130-900 cm^{-1} are assigned to stretching and deformation vibrations of metal-oxygen bonds. The majority of these lines in the hydroxides are splitted as a result of considerable distortion of MO_6 octahedra when lithium ions are replaced by protons. On the spectrum of titanium hydroxide H_2TiO_3 two lines are observed in the region of stretching vibrations of O-H bonds (2500 – 4000 cm^{-1}). The broad line can be attributed to hydrogen-bonded OH groups, whereas the narrow line – to isolated OH groups, which do not interact with other oxygen-hydrogen groups.

A wide asymmetric line is observed in the spectrum of zirconium hydroxide H_2ZrO_3. Its asymmetric shape is evidence of two types of structural OH groups having slightly different binding energies with the crystal lattice, in

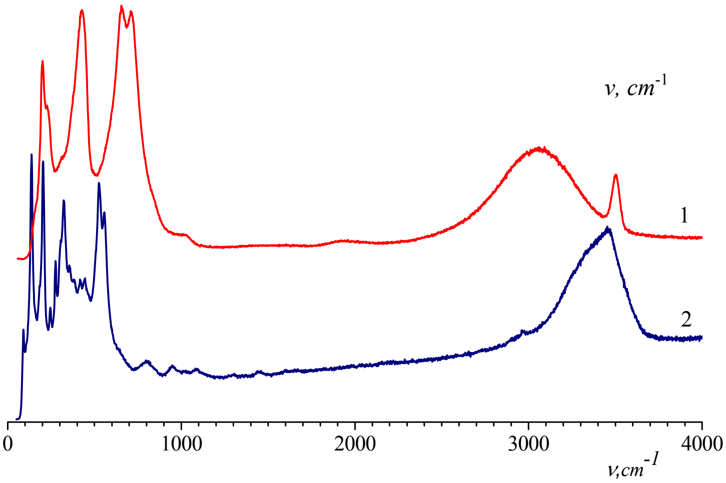

Fig. 6. Raman spectra for H_2TiO_3 (1), H_2ZrO_3 (2)

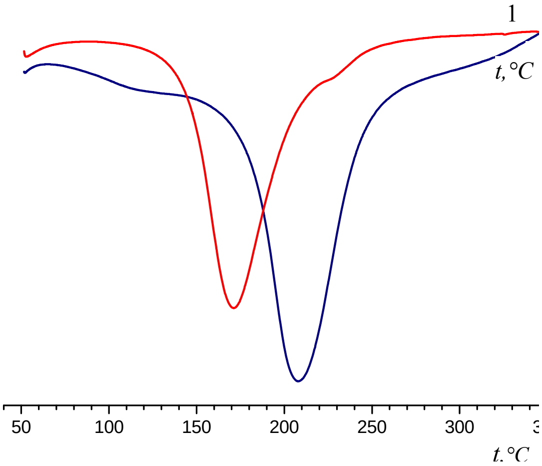

Fig. 7. TDG curves for H_2TiO_3 (1), H_2ZrO_3 (2) samples

conformity with two lithium ion sites in the initial lithium zirconate, which are occupied by protons. The stretching vibration line in the spectrum of H_2ZrO_3 is shifted to a higher-frequency region as compared with H_2TiO_3. Therefore, protons in H_2ZrO_3 are stronger bonded with oxygen atoms and form weaker hydrogen bonds than in the titanium hydroxide H_2TiO_3. As a consequence thermal stability of H_2ZrO_3 slightly exceeds the one of H_2TiO_3. The temperature of decomposition effect maximum for zirconium hydroxide is (450 - 470) K and approximately by 20° higher then one for titanium hydroxide (Fig.7). The dehydration effect maxima for hydrated zirconium and titanium dioxides occur at lower temperatures, approximately at 400 K, since almost all oxygen-hydrogen groups are located on the surface of dioxide particles.

To summarize, we have shown that almost all protons of zirconium and titanium hydroxide are structural and only a small part of them belong to absorbed water molecules. All protons in zirconium hydroxide belong to hydrogen-bonded OH-groups. Titanium hydroxide contains both hydrogen-bonded and isolated OH-groups. Protons in H_2ZrO_3 form hydrogen bonds weaker than in H_2TiO_3.

References

1. Pletnev R. N., Ivakin A. A., Kleshchev D. G., et al., *Hydrated Oxides of the Group IV and V Elements* (Nauka, Moscow, 1986) (*in Russian*).
2. Ou H, Lo S. *Separat. and Purif. Technol.* **58**, 179 (2007).
3. Pantyukhina M.I., Andreyeva O.L., Zubkov V.G., Tyutyunnik A.P. *Zhurn. Neorg. Khimii*. **46**, 1716 (2001) (*in Russian*)
4. Dorrian, J.F,. Newnham R. E. *Mater. Res. Bull.* **4**, 179 (1969).
5. Hodeau J.L., Marezio M. *J. of Solid State Chem*. **45**, 170 (1982).
6. Abragam A., *The Principles of Nuclear Magnetism* (Clarendon Press, Oxford, 1961).
7. Haeberlen U., Mahring M., *High Resolution NMR Spectroscopy in Solids* (Mir, Moscow, 1980) (*in Russian*).
8. Brandmüller J., Moser H., *Einführung in die Ramanspektroskopie* (Mir, Moscow, 1964) (*in Russian*).